Article:

van Veen, B., Montefiori, E., Modenese, L. et al. (2 more authors) (2019) Muscle recruitment strategies can reduce joint loading during level walking. Journal of Biomechanics, 97. 109368. ISSN 0021-9290

https://doi.org/10.1016/j.jbiomech.2019.109368

Journal of Biomechanics 97 (2019) 109368

Contents lists available at ScienceDirect

Journal of Biomechanics

journal homepage: www.elsevier.com/locate/jbiomech
www.JBiomech.com

Muscle recruitment strategies can reduce joint loading during level walking

Bart van Veen [a], Erica Montefiori [a], Luca Modenese [a,b], Claudia Mazzà [a,*], Marco Viceconti [c,d]

[a] Department of Mechanical Engineering and INSIGNEO Institute for in Silico Medicine, University of Sheffield, UK
[b] Department of Civil and Environmental Engineering, Imperial College London, UK
[c] Department of Industrial Engineering, Alma Mater Studiorum - University of Bologna, Italy
[d] Medical Technology Lab, Rizzoli Orthopaedic Institute, Bologna, Italy

ARTICLE INFO

Article history:
Accepted 22 September 2019

Keywords:
Neuromuscular control
Muscle recruitment
Joint load
Level walking
Musculoskeletal modelling

ABSTRACT

Joint inflammation, with consequent cartilage damage and pain, typically reduces functionality and affects activities of daily life in a variety of musculoskeletal diseases. Since mechanical loading is an important determinant of the disease process, a possible conservative treatment is the unloading of joints. In principle, a neuromuscular rehabilitation program aimed to promote alternative muscle recruitments could reduce the loads on the lower-limb joints during walking. The extent of joint load reduction one could expect from this approach remains unknown. Furthermore, assuming significant reductions of the load on the affected joint can be achieved, it is unclear whether, and to what extent, the other joints will be overloaded. Using subject-specific musculoskeletal models of four different participants, we computed the muscle recruitment strategies that minimised the hip, knee and ankle contact force, and predicted the contact forces such strategies induced at the other joints. Significant reductions of the peak force and impulse at the knee and hip were obtained, while only a minimal effect was found at the ankle joint. Adversely, the peak force and the impulse in non-targeted joints increased when aiming to minimize the load in an adjacent joint. These results confirm the potential of alternative muscle recruitment strategies to reduce the loading at the knee and the hip, but not at the ankle. Therefore, neuromuscular rehabilitation can be targeted to reduce the loading at affected joints but must be considered carefully in patients with multiple joints affected due to the potential adverse effects in non-targeted joints.

1. Introduction

Joint damage or inflammation and consequent pain typically reduce functionality and affect activities of daily life in a variety of musculoskeletal diseases. Associated altered joint loading might considerably affect damage progression within the joint cartilage and even the underlying bone. Indeed, aberrant loading of joints has been identified as an important risk factor of the progression of knee osteoarthritis (Waller et al., 2011) due to a number of factors, including varus-valgus misalignment and anterior cruciate ligament rupture (Andriacchi et al., 2004; Brouwer et al., 2007; Sharma et al., 2001). Even though this is still a contentious topic (Felson, 2000; Reijman et al., 2006), excessive joint loading as a result of obesity has been related to joint degeneration as reported for hip osteoarthritis (Cooper et al., 1998), total hip replacement (Karlson et al., 2003) and tibiofemoral misalignment (Felson et al., 2004).

Unloading of joints has been proposed as a conservative treatment to osteoarthritis progression (Lafeber et al., 2006) and interventions focus on weight loss and gait retraining (Shull et al., 2013). In contrast, selective strength training and neuromuscular rehabilitation (Brosseau et al., 2017) do not aim to introduce macroscopic kinematic compensations in the gait pattern, but rather to develop subtler neuromotor strategy compensations. Physical interventions, designed to reduce the load transmitted to the affected joint by modifying the neuromuscular recruitment patterns during gait, have a high potential because muscle forces are the primary contributors to joint compressive forces (Winby et al., 2009; Winter, 2009). However, one may wonder if it is reasonable to expect a significant reduction in the force transmitted through a joint by simply modifying the muscular recruitment strategy while preserving the gait kinematics, as it is also the least invasive of the interventions.

Musculoskeletal models offer a valuable non-invasive solution to investigate the forces transmitted at joints during activities of daily life. A common assumption in these models is that the central

* Corresponding author.
E-mail address: c.mazza@sheffield.ac.uk (C. Mazzà).

https://doi.org/10.1016/j.jbiomech.2019.109368
0021-9290/

nervous system solves an optimization problem to solve the muscle load-sharing problem. Different plausible muscle recruitment strategies in walking have been proposed (Anderson and Pandy, 2001; Crowninshield and Brand, 1981; Erdemir et al., 2007; Seireg and Arvikar, 1975). The minimization of the sum of muscle activations squared was shown to be equivalent to energetically optimal strategies and is now widely used to estimate muscle forces in simulations of gait (Anderson and Pandy, 2001). However, a previous optimization study showed that alternative neuromotor control could significantly reduce axial knee loads on the tibia throughout the stance phase of gait (DeMers et al., 2014), while an exploration of possible muscle recruitment strategies in walking suggested that the potential to reduce the hip loads might be limited (Martelli et al., 2011). The load-reducing potential of alternative muscle recruitment remains unknown for the ankle. In addition, the influence of alternative muscle recruitment strategies on the load in adjacent joints has not been investigated. The current study hence aimed to fill these gaps by answering the following questions: (1) Can alternative muscle recruitment strategies reduce the peak contact force and the impulse transmitted at each lower limb joint during level walking? (2) If a muscle recruitment strategy that significantly reduces the force in one joint exists, what is its influence on the other joints? (3) What muscle groups are involved in strategies that could reduce the force at the joints of the lower limb? In order to strengthen and broaden the scope of the study, we attempted to falsify the hypothesis that the muscle recruitment strategies that reduce joint contact forces would replicate in highly diverse subjects in terms of age, gender, weight and health status and in diverse types of musculoskeletal models.

2. Methods

2.1. Experimental data

Four subject-specific musculoskeletal models of the following participants (Table 1) were included in the study: a healthy participant (*p01*), a participant with an instrumented full right knee replacement (*p02;* sixth Knee Grand Challenge dataset (Fregly et al., 2012)), a participant with juvenile idiopathic arthritis (*p03;* (Montefiori et al., 2019)) and a participant with osteopenia (*p04;* (Montefiori et al., 2018)). The models were scaled from a generic model (*p01*) or built using NMSBuilder (Valente et al., 2017) following different approaches. Inverse dynamics simulations were run in OpenSim (Delp et al., 2007), driven with data collected from different laboratories.

Overground level-walking trials recorded at a self-selected (all participants) and slow and fast (*p01* and *p04*) speeds were investigated (Table 2). Three-dimensional positions of skin markers and ground reaction forces were available for all trials. Technical details of the data collection, different for each participant, are provided in the supplementary material. A 10 Hz low-pass, zero-lag, 4th order Butterworth filter was applied to the ground reaction force and centre of pressure trajectories. For the time points with a vertical reaction force below 20 N, the force and centre of pressure components were set to zero.

2.2. Musculoskeletal models

The musculoskeletal models included in this study were constructed following different pipelines (Table 3). For *p01*, *p02* and *p03*, the initial maximal isometric muscle forces were taken from the same generic model (Delp et al., 1990). The maximal isometric forces were scaled uniformly according to the ratio between the lower-limb mass of the participant and the generic model. After the initial muscle force scaling, the model of *p01* appeared too weak to produce the required torques of the fast walking trials. The maximal isometric forces were increased by a factor 1.5, as the characteristics of the specimens used to define the muscle parameters of the generic model differed substantially from those of *p01*, who was a healthy, young adult (Brand et al., 1986; Yamaguchi, 2001). For *p04*, the maximal isometric forces (F_{max}) for the muscles, that were visible in the MRI images, were estimated based on the muscle volumes segmented from the images:

$$F_{max} = k * \frac{V}{l_{opt}} \quad (1)$$

where k is the specific tension (61 N/cm^2, (Delp et al., 1990)), V is the muscle volume and l_{opt} is the optimal muscle fibre lengths as defined in the generic model. The pennation angles were also taken from the generic model. The muscle force-length-velocity relationship was not considered for any of the participants.

Table 1
Details of participants.

	Gender	Age (yrs.)	Height (m)	Mass (kg)
p01	male	28	1.90	82
p02*	male	unknown	1.72	70
p03	female	16	1.68	83
p04	female	74	1.64	57

* Participant has a total knee replacement in the right limb.

Table 2
Number of available trials (#) and average walking speeds for each participant.

	Self-selected		Slow		Fast	
	#	Speed ± SD (m/s)	#	Speed ± SD (m/s)	#	Speed ± SD (m/s)
p01	6	1.24 ± 0.02	5	1.03 ± 0.05	2	2.43 ± 0.06
p02	6	1.03 ± 0.02	N/A	N/A	N/A	N/A
p03	5	1.32 ± 0.03	N/A	N/A	N/A	N/A
p04	5	1.27 ± 0.03	5	1.14 ± 0.04	5	1.60 ± 0.05

Table 3
Details of musculoskeletal models: Scaled, generic (ScaGen) or subject-specific (SubSpec) model; Right lower limb (R), left lower limb (L) and/or head-arm-trunk segments (HAT) included; Number of segments, degrees of freedom (DoFs) and actuators included; Image types used to identify bone geometries, segment mass properties and orientations of joint axes; References to datasets and/or modelling pipelines.

	Model type	Body parts	No. of segments	No. of DoFs	No. of actuators	Images	References
p01	ScaGen	R, L, HAT	8	19	92	–	Delp et al., 1990, Lamberto et al., 2017
p02	SubSpec	R	5	11	43	CT + point-cloud	Fregly et al., 2012, Lin et al., 2010
p03	SubSpec	R	5	12	42	MRI	Modenese et al., 2018, Montefiori et al., 2019
p04	SubSpec	R, L	7	16	86	MRI	Montefiori et al., 2018

Fig. 1 shows the four different musculoskeletal models used in this study. Details of the model identification are provided in the supplementary material.

2.3. Inverse dynamics simulations

The generalized coordinates, $\vec{q}(t)$, were obtained by solving the inverse kinematics problem with a global optimization method (Lu and O'Connor, 1999) and subsequently filtered with a 10 Hz low-pass, zero-lag, 4th order Butterworth filter. The known generalized coordinates, velocities and accelerations were used to solve the equations of motion for the unknown torques (Delp et al., 2007). The trajectories of the generalized coordinates, forces and moments over the gait cycle are shown in the supplementary material.

2.4. Joint contact forces

The joint contact forces were computed following the implementation of joint reaction forces in OpenSim through MATLAB (Steele et al., 2012). The contact forces were computed as acting from the proximal segment on the distal segment at the joint centres, for which the definition can be found in the supplementary material. The primary outcome variable in this study was the peak magnitude of the joint contact forces, referred to in the results section as the peak force.

2.5. Muscle activations

Two objective functions within a constrained, nonlinear optimization were used to solve the muscle redundancy problem:

$$\begin{aligned} &\min && J\left(\vec{a}\right) \\ &\text{subject to} && \vec{T}(t) = B(q)\left(\vec{a}^{\,T}(t)\vec{F}_{max}\right) \\ & && 0 \leqslant \vec{a}(t) \leqslant 1 \end{aligned} \tag{2}$$

where $\vec{a}$ is the vector of activations with its entries defined as $a_i(t) = F_i(t)/F_{max,i}$, $\vec{F}_{max}$ is the vector of m maximum actuator forces, F_i is the force of actuator i, $\vec{T}$ is the $n \cdot 1$ vector of forces and moments of force acting at the generalized coordinates and B is the $n \cdot m$ matrix of muscle moment arms. The variables required to define the optimization problem were obtained using the OpenSim API through MATLAB (v2017a, The MathWorks Inc., Natick, MA, USA).

2.6. Objective functions

The first objective function, aimed to minimize overall muscle activation, was defined as:

$$J_{act}(\vec{a}) = \sum_{i=1}^{m} (a_i(t))^2 \tag{3}$$

where a_i is the activation of actuator i.

The second objective function, aimed to minimize the magnitude of the joint contact force, was defined as:

$$J_{Fj}(\vec{a}) = w_1\left(\frac{\|\vec{F^j}\left(\vec{a},t\right)\|}{\|\vec{F}^j_{act}\left(\vec{a}_{act},t\right)\|}\right) + w_2 R(\vec{a},t) \tag{4}$$

where $\|\vec{F^j}(\vec{a},t)\|$ is the magnitude of the contact force at joint j acting on its distal segment, $\|\vec{F}^j_{act}(\vec{a}_{act},t)\|$ is the magnitude of the contact force given the solution, $\vec{a}_{act}(t)$, of J_{act}, $R(\vec{a},t)$ is a regularization term to prevent the problem from being ill-posed (Tikhonov and Glasko, 1965) and w_1 and w_2 are constant weights that define the relative contribution of both parts to the objective function.

Without the regularization term R the cost function would be underdetermined, because the activation of the muscles that did not span the targeted joint would not be included. Therefore, the solution could vary along certain dimensions, or activations of muscles that did not span the targeted joint, without changing the value of the objective function. To ensure the optimization problem would have a unique solution, the regularization term was defined as:

$$R(\vec{a},t) = \frac{\sum_{i=1}^{m}\left(a_i^{NS}(t)\right)^2}{m} \tag{5}$$

where $a_i^{NS}(t)$ is the activation of the i^{th} muscle that did not span the joint for which the contact force was minimized. The ratio of the two weight constants, $w_1 : w_2$, was set to 10:1 such that the influence of the regularization term on the solution was negligible

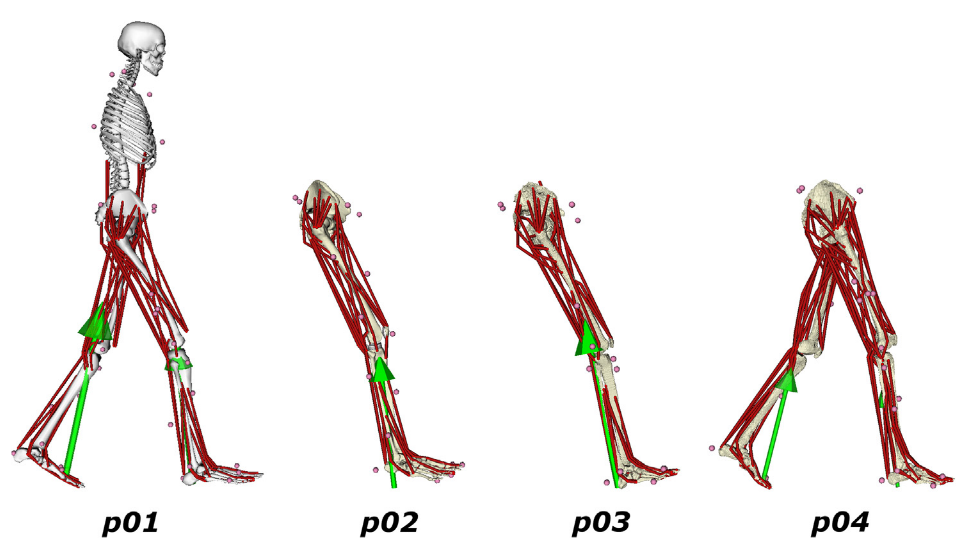

Fig. 1. The four different models during the loading phase of the right limb. The pink markers show the location of the model markers. The green arrows represent the ground reaction forces acting on the foot segments of the models. (For interpretation of the references to colour in this figure legend, the reader is referred to the web version of this article.)

(results from a sensitivity analysis of the resulting joint contact force to the weight ratio can be found in the supplementary material). Both the joint contact force term and the regularization term were normalized to keep their value between 0 and 1.

For each trial of each participant, the optimization problem was solved once for J_{act} and three times for J_{Fj}; once for the hip (J_{FH}), once for the knee (J_{FK}) and once for the ankle (J_{FA}). All optimizations were performed in MATLAB and details are provided in the supplementary material.

For those time points during the swing phase when $\|\vec{F}^{j}_{act}(\vec{a}_{act}, t)\|$ was null, no minimization of $J_{Fj}(\vec{a})$ for the corresponding joint was performed to avoid division by zero in the first part of the objective function. Therefore, no muscle activation values from the $J_{Fj}(\vec{a}, t)$ solution at these time points were included in any further analyses.

3. Results

The muscle recruitment strategy aimed to minimize the loads at the respective joints (J_{Fj}) reduced the peak magnitude of contact force and the impulse at the hip, knee and ankle compared to a recruitment strategy aimed to minimize the sum of muscle activa-

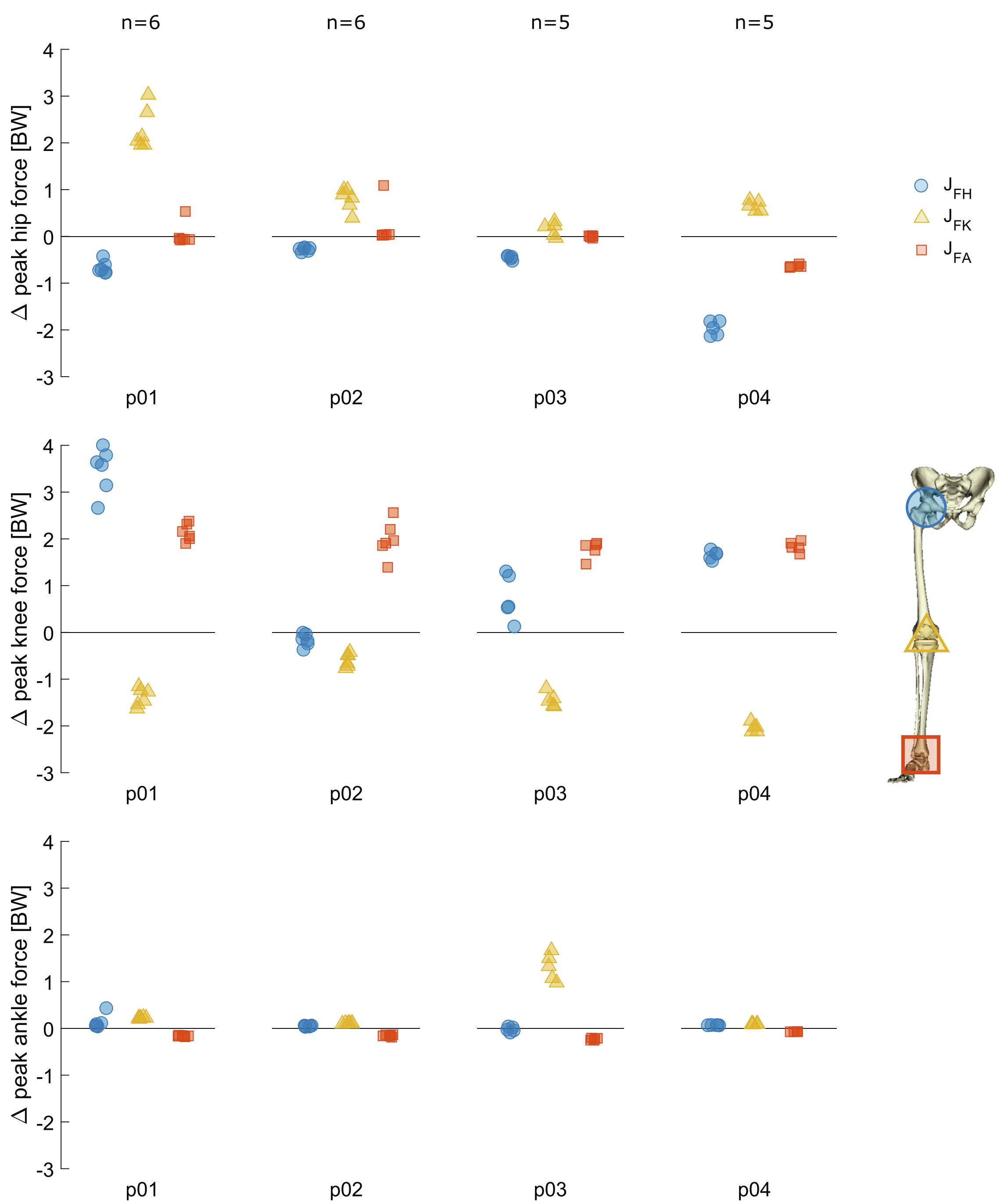

Fig. 2. The differences in peak contact force magnitude at the hip (top), knee (middle) and ankle (bottom) in bodyweight (BW) for the minimization of the contact force in the hip (J_{FH}, blue circles), the knee (J_{FK}, yellow triangles) and the ankle (J_{FA}, red squares) compared to the minimization of activation (J_{act}) for all trials at a self-selected walking speed for all participants (*p01*, *p02*, *p03* and *p04*). A negative value indicates a reduction in peak joint contact force magnitude compared to J_{act}. (For interpretation of the references to colour in this figure legend, the reader is referred to the web version of this article.)

tion squared (J_{act}), for all participants at a self-selected walking speed. The reduction of the peak contact force (Fig. 2), averaged over trials, ranged from $0.3 \pm 0.4 \cdot 10^{-1}$ (*p02*) to 2.0 ± 0.2 bodyweight (BW; *p04*) at the hip, from 0.6 ± 0.1 (*p02*) to 2.0 ± 0.1 BW (*p04*) at the knee and from $0.1 \pm 0.1 \cdot 10^{-2}$ (*p04*) to $0.2 \pm 0.2 \cdot 10^{-1}$ BW (*p03*) at the ankle depending on the participant. The reduction of impulse (Fig. 3), averaged over trials, ranged from $0.2 \pm 0.3 \cdot 10^{-1}$ (*p02*) to $0.6 \pm 0.3 \cdot 10^{-1}$ (*p04*) BW·s at the hip, from $0.4 \pm 0.5 \cdot 10^{-1}$ (*p02*) to 0.7 ± 0.1 (*p03*) BW·s at the knee depending on the participant and was up to $0.1 \pm 0.1 \cdot 10^{-1}$ BW·s at the ankle for all participants.

The effect that minimizing the load in one joint had on the peak magnitude of the contact force and the impulse in a non-targeted joint, compared to the J_{act} solutions, depended on both the participant and the joints involved (Figs. 2 and 3). No influence of the walking speed on the changes in joint contact forces could be observed.

For *p02*, who had an instrumented knee implant, the predicted knee forces from J_{act} were similar in terms of magnitude to the measured values. For *p01*, *p03* and *p04*, the predicted average peak knee forces from J_{act} were higher than for *p02* (Fig. 4).

When aiming to minimize the hip contact force, at the time instant of peak hip force, the activation of the *gluteus minimus* compartments and the *gracilis, sartorius* and *tensor fasciae latae* muscles, three knee stabilizers, increased, while the activation of the *gluteus medius* compartments and the *iliopsoas* muscles decreased.

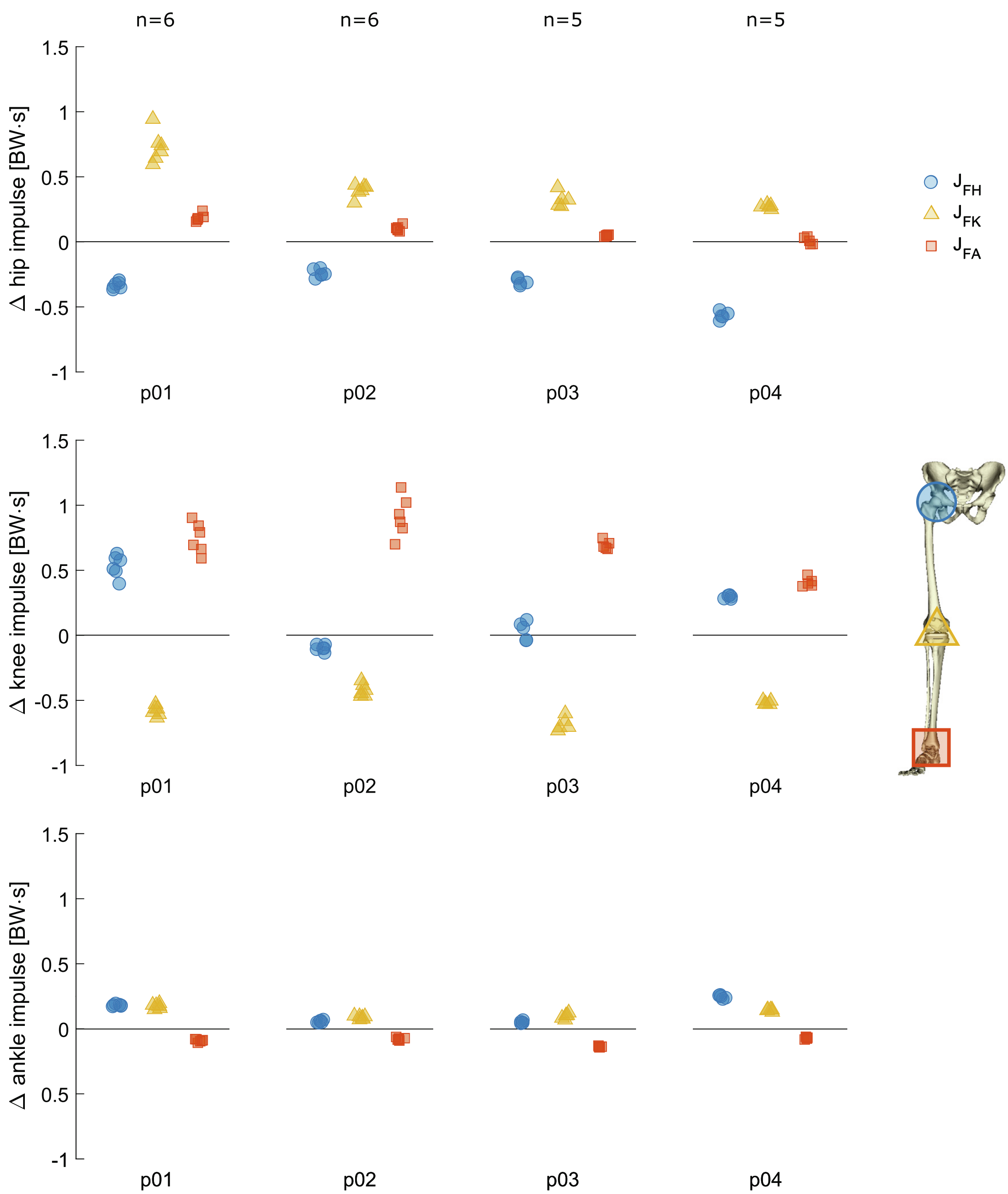

Fig. 3. The differences in impulse at the hip (top), knee (middle) and ankle (bottom) in bodyweight second (BW·s) for the minimization of the contact force in the hip (J_{FH}, blue circles), the knee (J_{FK}, yellow triangles) and the ankle (J_{FA}, red squares) compared to the minimization of activation (J_{act}) for all trials at a self-selected walking speed for all participants (*p01*, *p02*, *p03* and *p04*). A negative value indicates a reduction in peak joint contact force magnitude compared to J_{act}. (For interpretation of the references to colour in this figure legend, the reader is referred to the web version of this article.)

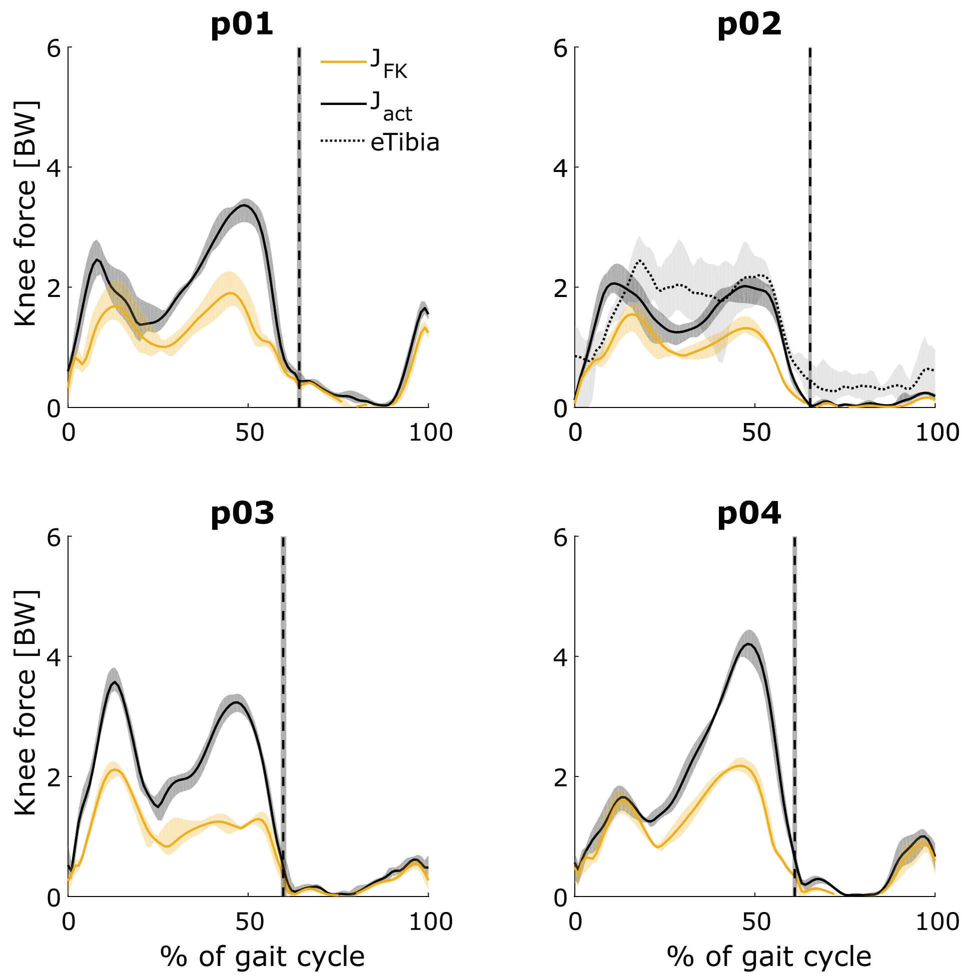

Fig. 4. Knee contact force trajectories of all participants for the trials at a self-selected walking speed; mean (solid line) and range (shaded area) values of force magnitude are shown in bodyweight (BW) for the J_{act} (black) and J_{FK} (yellow) solutions. For *p02*, the mean and range values as measured by the implant (*eTibia*, dotted) are shown. The vertical dashed line indicates the time instant when toe off occurred. (For interpretation of the references to colour in this figure legend, the reader is referred to the web version of this article.)

For three out of four participants, the activation of the *rectus femoris* and *gemellus* muscle increased and a shift in activation from the *soleus* to the *gastrocnemius* muscles occurred (Fig. 5).

When aiming to minimize the knee contact force, at the time instant of peak knee force, the activation of the *gluteus medius* (and, to a lesser extent, *the gluteus minimus*) compartments, the *iliopsoas* muscles, and the *soleus* muscle increased. The *rectus femoris* muscle, the knee stabilizers and the *gastrocnemius* muscles (except for the lateral compartment of *p04*) were switched off. For *p01* and *p02*, the *semitendinosus* muscle became involved, while for *p03* the activation of the smaller plantarflexor muscles around the ankle increased (Fig. 5). These changes in muscle activation patterns were consistent across participants even though the peak loads for the J_{act} solution, in both the hip and the knee joint, occurred predominantly during late stance for *p01* and *p04* and predominantly during early stance for *p02* and *p03* (see supplementary materials).

When aiming to minimize the ankle contact force, at the time instant of peak ankle force, the activation of the *soleus* muscle decreased, while the activation of the *gastrocnemius* and the *rectus femoris* (and to a lesser extent the *iliopsoas*) muscles increased.

4. Discussion

This study explored the potential of alternative muscle recruitment strategies to reduce the forces experienced by the joints of the lower limb during level walking. The peak joint contact force and impulse were assessed, firstly, to investigate the effectiveness of such strategies at the targeted joints and, secondly, to investigate potential adverse effects on the non-targeted joints. Lastly, the muscle groups involved in joint load reducing strategies were identified.

Alternative recruitment strategies reduced the peak contact force and the impulse in the knee and hip compared to the minimization of the sum of muscle activation squared (J_{act}). The effect on the peak force and the impulse reached up to 47% in the knee and up to 21% in the hip, while the effect on the ankle was minimal. The reduction in hip contact force did not exceed the maximum value (3.8 BW) reported in a previous study into the effect of alternative muscle recruitment strategies on the hip contact force (Martelli et al., 2011). The largest reduction of peak force at the knee (2.0 ± 0.1 BW for *p04*) was smaller than that reported in a previous study (3.2 BW), which overestimated the measured knee contact force when minimizing overall muscle activation (DeMers et al., 2014). The largest reduction of knee contact force occurred during late stance, particularly for *p01, p03* and *p04*, in accordance to results from a previous study (DeMers et al., 2014). The authors of this study argued that a smaller net moment at the knee during late stance compared to early stance allowed for a larger variability in muscle activation around the knee and hence a larger variability of knee contact force. However, in the current study the net knee moment was not consistently smaller during

Fig. 5. Muscle activations for the J_{act} and the J_{FH}, J_{FK} and J_{FA} solutions at the time of peak hip, knee and ankle contact force magnitude in the J_{act} solution (t_{FHmax}, t_{FKmax} and t_{FAmax}, respectively). Muscle activation values are averaged over trials at self-selected walking speed and represented by a colour scale (white: no activation, red: full activation). For each muscle, the four rows represent the activation level for the different participants. Thus, the first column compares the muscle activations from J_{act} to those from J_{FH} at the time point when the hip contact force magnitude was maximal in the J_{act} solution. The second and third column represent the same comparison for the knee and ankle, respectively. (For interpretation of the references to colour in this figure legend, the reader is referred to the web version of this article.)

late stance than during early stance across the four models. The larger net ankle moment during push-off compared to early stance might provide an alternative explanation: when minimizing overall muscle activation, the mono-articular soleus and the bi-articular gastrocnemius share the load. However, when minimizing the knee contact force, the soleus, being mono-articular, provides the required plantarflexion moment at the ankle without loading the knee. In general, these results suggest that the knee and, to a lesser extent, the hip should be targeted by conservative treatments that aim to unload joints.

A muscle recruitment strategy that minimised the force in a specific joint increased the force in an adjacent joint. When aiming to minimize hip force, the peak force increased in the knee, but not in the ankle. When aiming to minimize knee force, the peak hip force and, to a lesser extent, the peak ankle force increased. When aiming to minimize the ankle force, the peak force increased in the knee, but not in the hip. This shift of load towards non-targeted joints was to be expected due to the coupling of the joints through multi-articular muscles. The effect of this compensation decreases when moving further away from the targeted joint along the kinematic chain. The magnitude of the adverse effects on the load in non-targeted joints, at a self-selected walking speed, was dependent on the joint and varied across participants, but should not be ignored. For example, the knee load, when minimizing the hip force, doubled from 3.4 to 6.8 BW for *p01*. These adverse effects are most likely sensitive to the capacity of muscles in the model to produce force beyond the minimum required by the dynamic equilibrium and should therefore be further investigated. In this study, we investigated the immediate effect of alternative muscle recruitment strategies on the magnitude of joint loading. Alternative muscle recruitment strategies could also affect joint stability and load distribution within the joints. However, other modelling approaches would be required to study these effects.

The potential of alternative muscle recruitment strategies to reduce joint contact forces and their adverse effects on non-targeted joints were measured against an estimated reference (J_{act}). For *p02*, who had an instrumented knee implant, the predicted knee forces from J_{act} were close to the measured values. For *p01*, *p03* and *p04*, the predicted peak forces in the hip and knee from J_{act} were higher than those measured with instrumented implants for *p02* and higher than in other studies (Bergmann et al., 2001; Damm et al., 2017; Kutzner et al., 2010). However, *p01*, *p03* and *p04* were either healthy or did not have a pathology with hip or knee involvement. Therefore, a notable difference in walking dynamics most likely exists with patients that underwent a full hip replacement. The low self-selected walking speed of *p02* supports the choice to use the J_{act} solutions as a reference.

The changes in muscle activation patterns depended on the joint in which the force was minimized: when the force in the hip was minimized, the peak hip force reduced due to a shift in activation from the *gluteus medius* to the *gluteus minimus* muscle and a decrease in the activation of the *iliopsoas* muscles. The *rectus femoris*, *sartorius* and *tensor fasciae latae* muscles maintained the levels of hip flexion and adduction moment during late stance (DeMers et al., 2014). The knee contact force increased due to the bi-articular nature of these muscles; when the knee force was minimized, a shift in activation from the bi-articular *rectus femoris* and *gastrocnemius* muscles to the mono-articular *iliopsoas* and *soleus* muscles reduced the peak knee force. The mono-articular muscles have a smaller moment arm and therefore a larger muscle force is required to produce the hip and ankle moments. Given the weight ratio of the cost function that aimed to minimize the contact force in a specific joint, the activation level of a multi-articular muscle that spans the targeted joint is determined by the joint contact force term. The influence of the activation term is minimal and therefore muscles that do not span the targeted joints are required to compensate; when minimizing the ankle force, the peak force in the ankle reduced only by a very small amount due to a shift in activation from the *soleus* to the *gastrocnemius* muscles. An increase in the activation of this bi-articular muscle increased the force experienced by the knee significantly. The above muscle groups should be considered in the design of conservative treatments, while considering the risk of fatigue due to increased activation of specific muscle groups. Overall, an alternative muscle recruitment strategy to reduce joint loads prefers to reduce muscle activation locally in contrast to a strategy that minimizes overall muscle activation, which is equivalent to an energetically optimal strategy (Anderson and Pandy, 2001).

The four participants represented widely different populations in terms of age (16–74 years old), height (1.64–1.90 m), mass (57–83 kg) and health status. The musculoskeletal models were identified on different levels of subject specificity, ranging from a scaled generic model (*p01*) to a model with fully personalised musculoskeletal geometry and joint orientation (*p04*). Nonetheless, the consistency of the results suggests the outcomes are not subject specific in their general nature, but are determined by the physical limitations in each of the lower limb joints as expressed through their dynamic equilibrium equations.

The main limitation of this study is the assumption that the central nervous system controls the muscles independently, while dependencies between the control of individual muscles might exist. For example, the concept of muscle synergies has been proposed to represent these dependencies, but the existence of such synergies is not without debate (Tresch and Jarc, 2009). The authors acknowledge that future work should assess whether the load reductions found in this study are achievable in practice, considering the potential dependencies in muscle control. Nonetheless, this study did provide a theoretical upper boundary to the reduction of joint loads, and the potential load increase in adjacent joints, one can expect to achieve through alternative muscle recruitment strategies. Secondly, the muscle force-length-velocity relationship was not considered when determining the force producing capacity of the muscles to avoid introducing a confounding factor due to the estimation of the subject-specific parameters. Lastly, results from this study are somehow limited in scope as they assume that the compensation strategy is limited to the neuromuscular control and not to possible changes in joint kinematics. Nonetheless, this assumption represents an idealised case, representative of moderately severe compensation strategies, typical of early-stage pathologies.

In conclusion, the results presented in this study suggest that alternative muscle recruitment strategies can reduce the loading of the affected joint at the knee and the hip. Instead, the ankle joint load can only be reduced by a small amount by simply changing the neuromuscular control. The *gluteus minimus*, *rectus femoris*, *sartorius* and *tensor fasciae latae* muscles were primarily involved in the reduction of the hip force, while the *iliopsoas* and *soleus* muscles were primarily involved in the reduction of knee contact force. These alternative muscle recruitment strategies come at a potential cost of moderate increase in the loading at other joints. Therefore, neuromuscular rehabilitation can be targeted to reduce the loading at affected joints but must be considered carefully in patients with multiple joints affected due to the potential adverse effects in non-targeted joints.

Data statement

The models, data and supplementary figures and material used in this study can be freely downloaded from Figshare (https://doi.org/10.15131/shef.data.5288311).

Declaration of Competing Interest

The authors declare that they do not have any financial or personal relationships with other people or organisations that could have inappropriately influenced this study.

Acknowledgements

This project was partly funded by the EPSRC Frontier Engineering Awards, United Kingdom Awards (Grant Reference No. EP/K03877X/1) and the European Commission MD-PAEDIGREE project (FP7-ICT Programme, Project ID: 600932) and partly carried out at the NIHR Sheffield Biomedical Research Centre (BRC), United Kingdom. The authors would like to thank Dr. Giuliano Lamberto for his help with the construction of the model for *p01*.

References

Anderson, F.C., Pandy, M.G., 2001. Static and dynamic optimization solutions for gait are practically equivalent. J. Biomech. 34, 153–161. https://doi.org/10.1016/S0021-9290(00)00155-X.

Andriacchi, T.P., Mündermann, A., Smith, R.L., Alexander, E.J., Dyrby, C.O., Koo, S., 2004. A framework for the in vivo pathomechanics of osteoarthritis at the knee. Ann. Biomed. Eng. 32, 447–457. https://doi.org/10.1023/B:ABME.0000017541.82498.37.

Bergmann, G., Deuretzbacher, G., Heller, M., Graichen, F., Rohlmann, A., Strauss, J., Duda, G., 2001. Hip contact forces and gait patterns from routine activities. J. Biomech. 34, 859–871. https://doi.org/10.1016/S0021-9290(01)00040-9.

Brand, R.A., Pedersen, D.R., Friederich, J.A., 1986. The sensitivity of muscle force predictions to changes in physiologic cross-sectional area. J. Biomech. 19, 589–596. https://doi.org/10.1016/0021-9290(86)90164-8.

Brosseau, L., Taki, J., Desjardins, B., Thevenot, O., Fransen, M., Wells, G.A., Imoto, A. M., Toupin-April, K., Westby, M., Gallardo, I.C.Á., Gifford, W., Laferrière, L., Rahman, P., Loew, L., Angelis, G. De, Cavallo, S., Shallwani, S.M., Aburub, A., Bennell, K.L., Van der Esch, M., Simic, M., McConnell, S., Harmer, A., Kenny, G.P., Paterson, G., Regnaux, J.-P., Lefevre-Colau, M.-M., McLean, L., 2017. The ottawa panel clinical practice guidelines for the management of knee osteoarthritis. Part one: introduction, and mind-body exercise programs. Clin. Rehabil. 31, 582–595. https://doi.org/10.1177/0269215517691083.

Brouwer, G.M., Tol, A.W. Van, Bergink, A.P., Belo, J.N., Bernsen, R.M.D., Reijman, M., Pols, H.A.P., Bierma-Zeinstra, S.M.A., 2007. Association between valgus and varus alignment and the development and progression of radiographic osteoarthritis of the knee. Arthritis Rheum. 56, 1204–1211. https://doi.org/10.1002/art.22515.

Cooper, C., Inskip, H., Croft, P., Campbell, L., Smith, G., Mclearn, M., Coggon, D., 1998. Individual risk factors for hip osteoarthritis: obesity, hip injury and physical activity. Am. J. Epidemiol. 147, 516–522. https://doi.org/10.1093/oxfordjournals.aje.a009482.

Crowninshield, R.D., Brand, R.A., 1981. A physiologically based criterion of muscle force prediction in locomotion. J. Biomech. 14, 793–801. https://doi.org/10.1016/0021-9290(81)90035-X.

Damm, P., Kutzner, I., Bergmann, G., Rohlmann, A., Schmidt, H., 2017. Comparison of in vivo measured loads in knee, hip and spinal implants during level walking. J. Biomech. 51, 128–132. https://doi.org/10.1016/j.jbiomech.2016.11.060.

Delp, S.L., Anderson, F.C., Arnold, A.S., Loan, P., Habib, A., John, C.T., Guendelman, E., Thelen, D.G., 2007. OpenSim: open-source software to create and analyze dynamic simulations of movement. IEEE Trans. Biomed. Eng. 54, 1940–1950. https://doi.org/10.1109/TBME.2007.901024.

Delp, S.L., Loan, J.P., Hoy, M.G., Zajac, F.E., Topp, E.L., Rosen, J.M., 1990. An interactive graphics-based model of the lower extremity to study orthopaedic surgical procedures. IEEE Trans. Biomed. Eng. 37, 757–767. https://doi.org/10.1109/10.102791.

DeMers, M.S., Pal, S., Delp, S.L., 2014. Changes in tibiofemoral forces due to variations in muscle activity during walking. J. Orthop. Res. 32, 769–776. https://doi.org/10.1002/jor.22601.

Erdemir, A., McLean, S., Herzog, W., van den Bogert, A.J., 2007. Model-based estimation of muscle forces exerted during movements. Clin. Biomech. 22, 131–154. https://doi.org/10.1016/j.clinbiomech.2006.09.005.

Felson, D.T., 2000. Osteoarthritis: new insights. Part 1: the disease and its risk factors. Ann. Intern. Med. 133, 635. https://doi.org/10.7326/0003-4819-133-8-200010170-00016.

Felson, D.T., Goggins, J., Niu, J., Zhang, Y., Hunter, D.J., 2004. The effect of body weight on progression of knee osteoarthritis is dependent on alignment. Arthrit. Rheum. 50, 3904–3909. https://doi.org/10.1002/art.20726.

Fregly, B.J., Besier, T.F., Lloyd, D.G., Delp, S.L., Banks, S.A., Pandy, M.G., D'Lima, D.D., 2012. Grand challenge competition to predict in vivo knee loads. J. Orthop. Res. 30, 503–513. https://doi.org/10.1002/jor.22023.

Karlson, E.W., Mandl, L.A., Aweh, G.N., Sangha, O., Liang, M.H., Grodstein, F., 2003. Total hip replacement due to osteoarthritis: the importance of age, obesity, and other modifiable risk factors. Am. J. Med. 114, 93–98. https://doi.org/10.1016/S0002-9343(02)01447-X.

Kutzner, I., Heinlein, B., Graichen, F., Bender, A., Rohlmann, A., Halder, A., Beier, A., Bergmann, G., 2010. Loading of the knee joint during activities of daily living measured in vivo in five subjects. J. Biomech. 43, 2164–2173. https://doi.org/10.1016/j.jbiomech.2010.03.046.

Lafeber, F.P., Intema, F., Van Roermund, P.M., Marijnissen, A.C., 2006. Unloading joints to treat osteoarthritis, including joint distraction. Curr. Opin. Rheumatol. 18, 519–525. https://doi.org/10.1097/01.bor.0000240366.54960.a1.

Lamberto, G., Martelli, S., Cappozzo, A., Mazzà, C., 2017. To what extent is joint and muscle mechanics predicted by musculoskeletal models sensitive to soft tissue artefacts? J. Biomech. 62, 68–72. https://doi.org/10.1016/j.jbiomech.2016.07.042.

Lin, Y.-C., Walter, J.P., Banks, S.A., Pandy, M.G., Fregly, B.J., 2010. Simultaneous prediction of muscle and contact forces in the knee during gait. J. Biomech. 43, 945–952. https://doi.org/10.1016/j.jbiomech.2009.10.048.

Lu, T.-W., O'Connor, J.J., 1999. Bone position estimation from skin marker co-ordinates using global optimisation with joint constraints. J. Biomech. 32, 129–134. https://doi.org/10.1016/S0021-9290(98)00158-4.

Martelli, S., Taddei, F., Cappello, A., van Sint Jan, S., Leardini, A., Viceconti, M., 2011. Effect of sub-optimal neuromotor control on the hip joint load during level walking. J. Biomech. 44, 1716–1721. https://doi.org/10.1016/j.jbiomech.2011.03.039.

Modenese, L., Montefiori, E., Wang, A., Wesarg, S., Viceconti, M., Mazzà, C., 2018. Investigation of the dependence of joint contact forces on musculotendon parameters using a codified workflow for image-based modelling. J. Biomech. 73, 108–118. https://doi.org/10.1016/j.jbiomech.2018.03.039.

Montefiori, E., Kalkman, B.M., Clarke, A., Paggiosi, M., McCloskey, E.V., Mazzà, C., 2018. A subject-specific musculoskeletal model to estimate joint loading at different walking speeds. Gait Post. 66, S28. https://doi.org/10.1016/j.gaitpost.2018.07.144.

Montefiori, E., Modenese, L., Di Marco, R., Magni-Manzoni, S., Malattia, C., Petrarca, M., Ronchetti, A., de Horatio, L.T., van Dijkhuizen, P., Wang, A., Wesarg, S., Viceconti, M., Mazzà, C., 2019. Linking joint impairment and gait biomechanics in patients with juvenile idiopathic arthritis. Ann. Biomed. Eng. https://doi.org/10.1007/s10439-019-02287-0.

Reijman, M., Pols, H.A.P., Bergink, A.P., Hazes, J.M.W., Belo, J.N., Lievense, A.M., Bierma-Zeinstra, S.M.A., 2006. Body mass index associated with onset and progression of osteoarthritis of the knee but not of the hip: the rotterdam study. Ann. Rheum. Dis. 66, 158–162. https://doi.org/10.1136/ard.2006.053538.

Seireg, A., Arvikar, R.J., 1975. The prediction of muscular load sharing and joint forces in the lower extremities during walking. J. Biomech. 8, 89–102. https://doi.org/10.1016/0021-9290(75)90089-5.

Sharma, L., Song, J., Felson, D.T., Cahue, S., Shamiyeh, E., Dunlop, D.D., 2001. The role of knee alignment in disease progression and functional decline in knee osteoarthritis. JAMA 286, 188–195. https://doi.org/10.1001/jama.286.2.188.

Shull, P.B., Silder, A., Shultz, R., Dragoo, J.L., Besier, T.F., Delp, S.L., Cutkosky, M.R., 2013. Six-week gait retraining program reduces knee adduction moment, reduces pain, and improves function for individuals with medial compartment knee osteoarthritis. J. Orthop. Res. 31, 1020–1025. https://doi.org/10.1002/jor.22340.

Steele, K.M., DeMers, M.S., Schwartz, M.H., Delp, S.L., 2012. Compressive tibiofemoral force during crouch gait. Gait Post. 35, 556–560. https://doi.org/10.1016/j.gaitpost.2011.11.023.

Tikhonov, A.N., Glasko, V.B., 1965. Use of the regularization method in non-linear problems. USSR Comput. Math. Math. Phys. 5, 93–107. https://doi.org/10.1016/0041-5553(65)90150-3.

Tresch, M.C., Jarc, A., 2009. The case for and against muscle synergies. Curr. Opin. Neurobiol. 19, 601–607. https://doi.org/10.1016/j.conb.2009.09.002.

Valente, G., Crimi, G., Vanella, N., Schileo, E., Taddei, F., 2017. NmsBuilder: freeware to create subject-specific musculoskeletal models for opensim. Comput. Meth. Progr. Biomed. 152, 85–92. https://doi.org/10.1016/j.cmpb.2017.09.012.

Waller, C., Hayes, D., Block, J.E., London, N.J., 2011. Unload it: the key to the treatment of knee osteoarthritis. Knee Surg. Sport. Traumatol. Arthrosc. 19, 1823–1829. https://doi.org/10.1007/s00167-011-1403-6.

Winby, C.R., Lloyd, D.G., Besier, T.F., Kirk, T.B., 2009. Muscle and external load contribution to knee joint contact loads during normal gait. J. Biomech. 42, 2294–2300. https://doi.org/10.1016/j.jbiomech.2009.06.019.

Winter, D.A., 2009. Biomechanics and Motor Control of Human Movement. John Wiley & Sons Inc, Hoboken, NJ, USA. https://doi.org/10.1002/9780470549148.

Yamaguchi, G.T., 2001. Appendix b: human lower extrimities muscle parameters. In: Dynamic Modeling of Musculoskeleton Motion. Springer US, Boston, MA, pp. 243–246. https://doi.org/10.1007/978-0-387-28750-8.